Electronic Supplementary Material (ESI) for Materials Horizons.

Supporting Information

Controllable Proton-Reservoir Ordered Gel towards Reversible Switching and Reliable Electromagnetic Interference Shielding

Yan-Qin Wang[1], Min Cao[1], Bo-Wen Liu[1], Fu-Rong Zeng[1], Qiang Fu[2], Hai-Bo Zhao[1]*, Yu-Zhong Wang[1]*

[1]Collaborative Innovation Center for Eco-Friendly and Fire-Safety Polymeric Materials (MoE), State Key Laboratory of Polymer Materials Engineering, National Engineering Laboratory for Eco-Friendly Polymer Materials (Sichuan), College of Chemistry, Sichuan University, Chengdu, 610064, China.

[2]College of Polymer Science and Engineering, State Key Laboratory of Polymer Materials Engineering, Sichuan University, Chengdu 610065, China.

*Corresponding authors. E-mail: haibor7@163.com; yzwang@scu.edu.cn; Fax: +86-28-85410259; Tel: +86-28-85410755

Supplemental Text

When the electromagnetic wave is incident on shielding materials, the sum of the reflection coefficient (R), absorption coefficient (A), and transmission coefficient (T) is 1. That is[1-3],

$$R + A + T = 1 \tag{S1}$$

The R and T coefficients are obtained from the network analyser in the form of scattering parameters.

$$R = |S_{11}|^2 = |S_{22}|^2 \tag{S2}$$

$$T = |S_{12}|^2 = |S_{21}|^2 \tag{S3}$$

The total EMI SE (SE_T) generally contributed from reflection (SE_R) and absorption (SE_A), which can be written as

$$SE_T = SE_A + SE_R \tag{S4}$$

$$SE_R = 10\log\left(\frac{1}{1-R}\right) = 10\log\left(\frac{1}{1-|S_{11}|^2}\right) \tag{S5}$$

$$SE_A = 10\log\left(\frac{1-R}{T}\right) = 10\log\left(\frac{1-|S_{11}|^2}{|S_{21}|^2}\right) \tag{S6}$$

The reflection and absorption in EMI shielding for multilayer materials can also be expressed as follows[4],

$$SE_R = 20\log\left(\frac{\sqrt{\mu_o\sigma}}{4\sqrt{2\pi f\mu\varepsilon_0}}\right) \tag{S7}$$

$$SE_A = 8.686d\sqrt{\pi f\mu\sigma} \tag{S8}$$

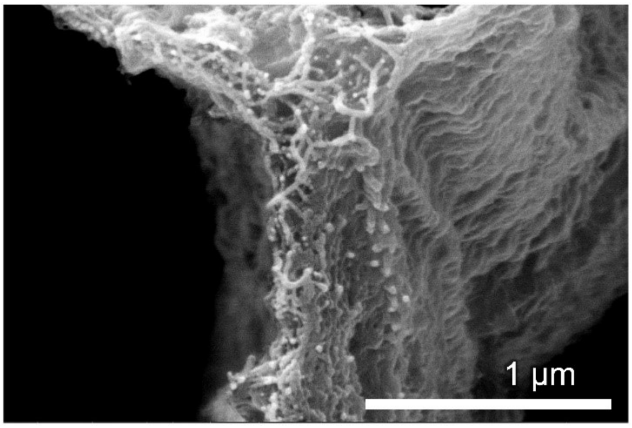

Figure S1. SEM image of PANI/SA aerogel.

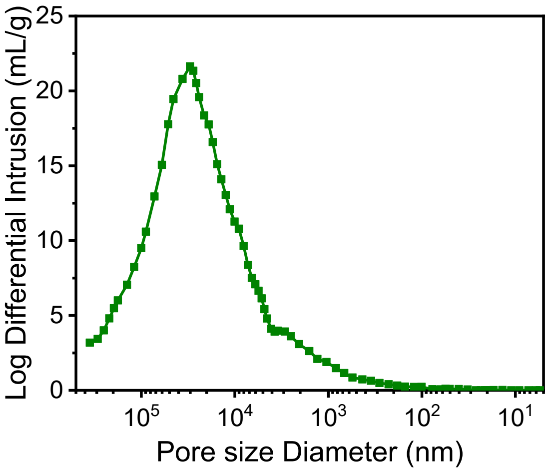

Figure S2. Pore diameter distribution of the PANI/SA aerogel.

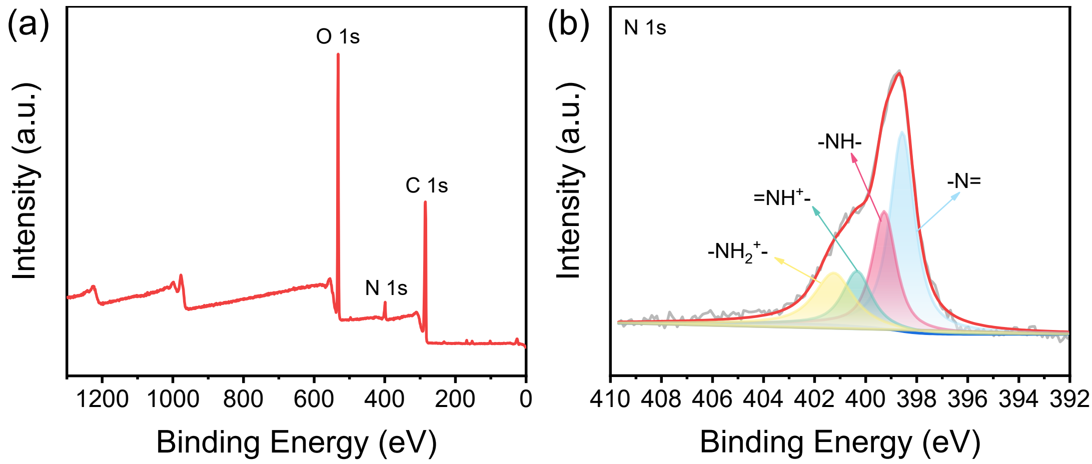

Figure S3. (a) XPS survey and (b) N 1s spectrum of PANI/SA aerogel.

Figure S4. Photograph of the PANI/SA hydrogel with editable arbitrary shape.

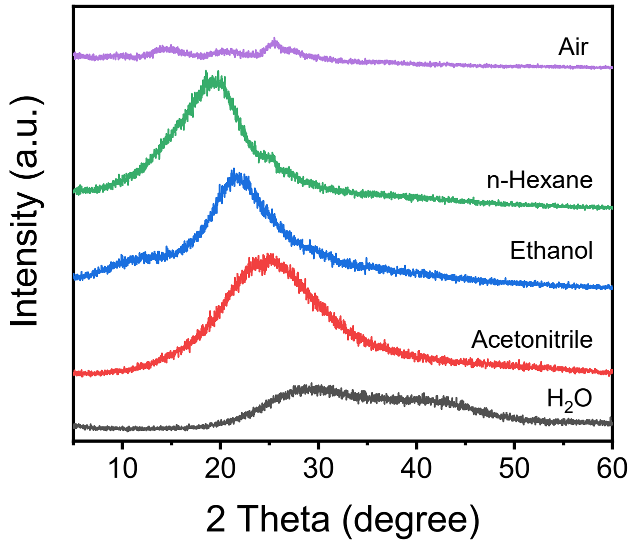

Figure S5. XRD patterns of PANI/SA gels.

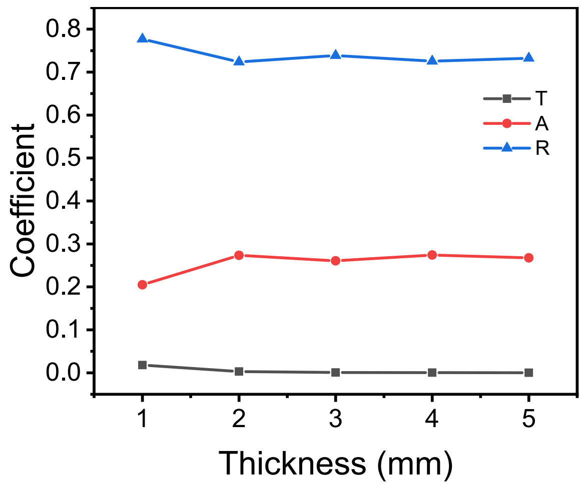

Figure S6. Power coefficients of PANI/SA hydrogels at different thicknesses.

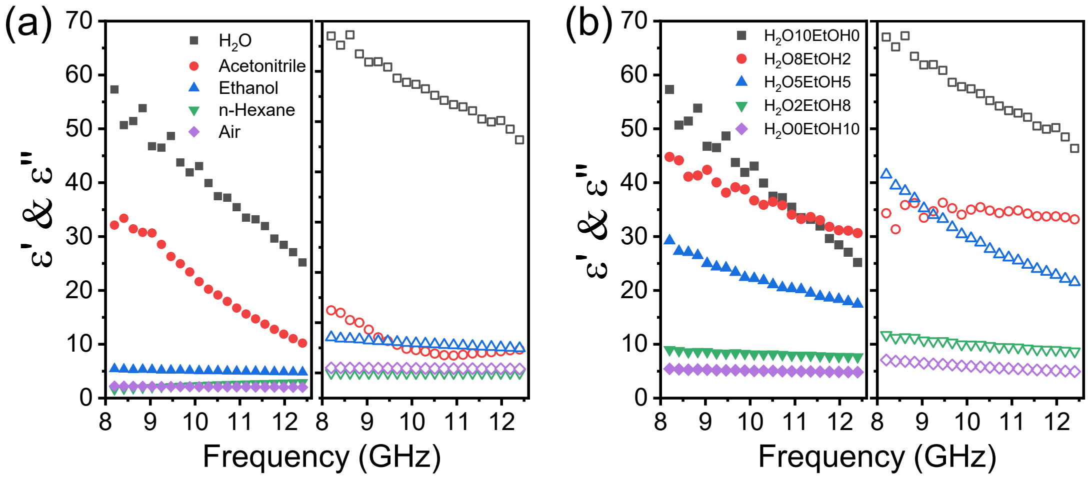

Figure S7. Complex permittivity of PANI/SA gels.

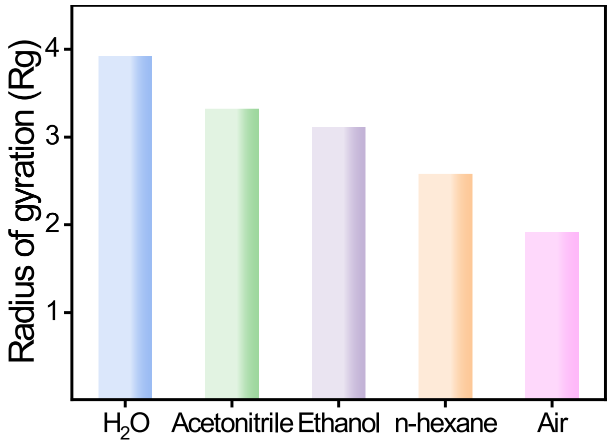

Figure S8. Radius of gyration of the PANI/SA gel in different solvent environments.

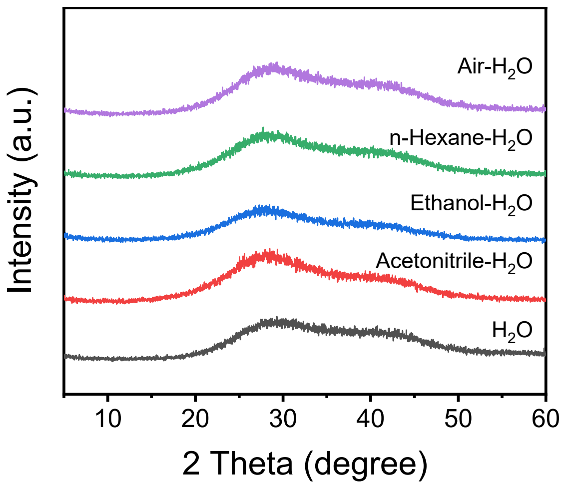

Figure S9. XRD patterns of PANI/SA hydrogels switched from organogels/aerogel.

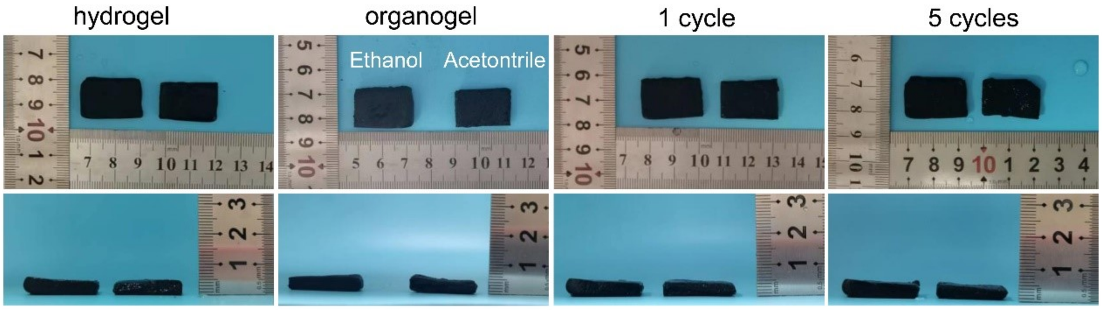

Figure S10. The volume evolution of PANI/SA gels during solvent displacement.

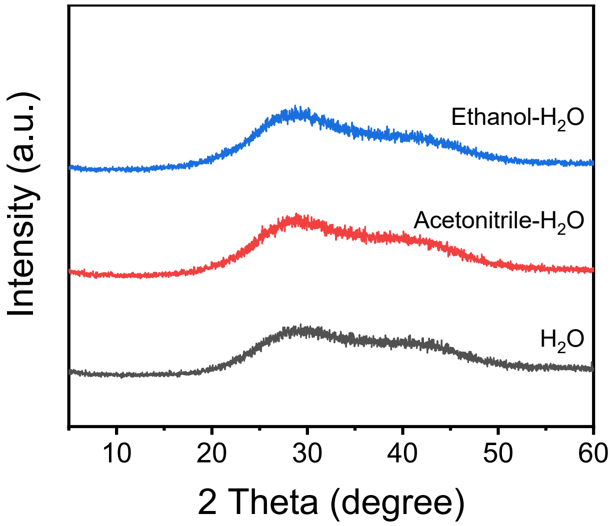

Figure S11. XRD patterns of the PANI/SA hydrogel after 5 solvent displacement cycles.

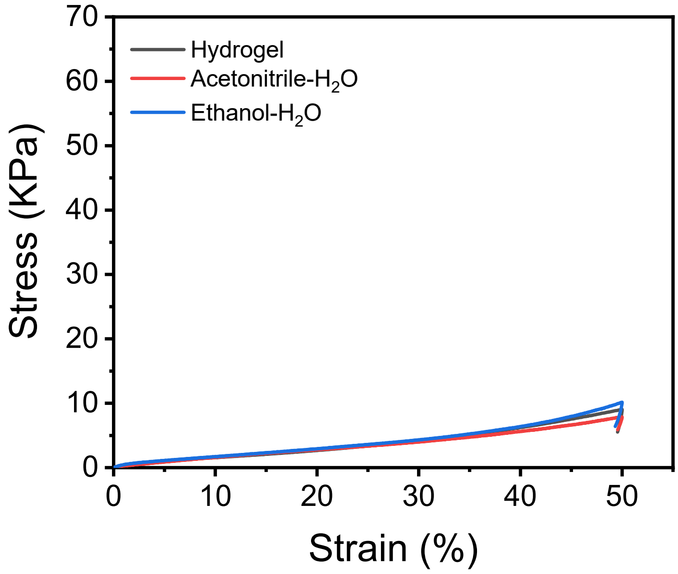

Figure S12. compression stress–strain curves of PANI/SA hydrogels after 5 solvent displacement cycles.

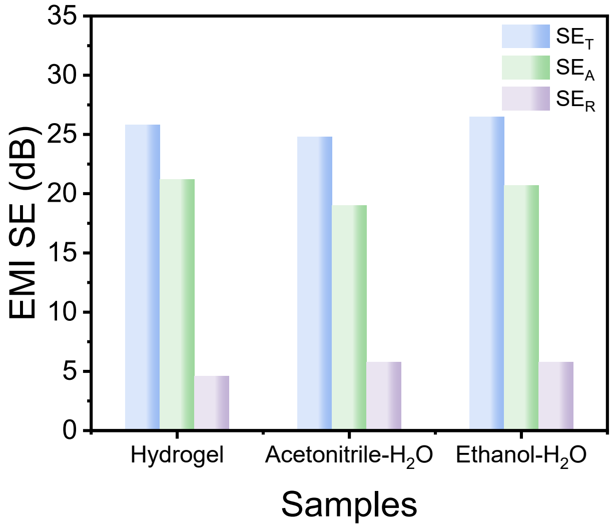

Figure S13. SE_A, SE_R, and SE_T of the PANI/SA hydrogels after 5 solvent displacement cycles.

References

1. F. Shahzad, M. Alhabeb, C. B. Hatter, B. Anasori, S. Man Hong, C. M. Koo and Y. Gogotsi, *Science*, 2016, **353**, 1137-1140.
2. X. Liu, Y. Li, X. Sun, W. Tang, G. Deng, Y. Liu, Z. Song, Y. Yu, R. Yu, L. Dai and J. Shui, *Matter*, 2021, **4**, 1735-1747.
3. Y. Yang, N. Wu, B. Li, W. Liu, F. Pan, Z. Zeng and J. Liu, *ACS Nano*, 2022, **16**, 15042-15052.
4. W.-L. Song, M.-S. Cao, M.-M. Lu, S. Bi, C.-Y. Wang, J. Liu, J. Yuan and L.-Z. Fan, *Carbon*, 2014, **66**, 67-76.